High Sensitive, Linear and Thermostable Pressure Sensor Utilizing Bipolar Junction Transistor for 5 kPa

Mikhail Basov (engineerbasovm@gmail.com)
Dukhov Automatics Research Institute (VNIIA) https://orcid.org/0000-0003-0798-4500

Research Article

Keywords: pressure sensor, bipolar junction transistor, differential amplifier, high sensitivity, low error

Posted Date: July 2nd, 2021

DOI: https://doi.org/10.21203/rs.3.rs-677110/v1

Version of Record: A version of this preprint was published at Physica Scripta on April 16th, 2021. See the published version at https://doi.org/10.1088/1402-4896/abf536.

High Sensitive, Linear and Thermostable Pressure Sensor Utilizing Bipolar Junction Transistor for 5 kPa

Mikhail Basov

Dukhov Automatics Research Institute (VNIIA), Moscow, Russia

E-mail: engineerbasovm@gmail.com

Received xxxxxx
Accepted for publication xxxxxx
Published xxxxxx

Abstract

Research of pressure sensor chip utilizing novel electrical circuit with bipolar-junction transistor-based (BJT) piezosensitive differential amplifier with negative feedback loop (PDA-NFL) for 5 kPa differential range was done. The significant advantages of developed chip PDA-NFL in the comparative analysis of advanced pressure sensor analogs, which are using the Wheatstone piezoresistive bridge, are clearly shown. The experimental results prove that pressure sensor chip PDA-NFL with 4.0x4.0 mm^2 chip area has sensitivity S = 11.2 ± 1.8 mV/V/kPa with nonlinearity of $2K_{NLback}$ = 0.11 ± 0.09 %/FS (pressure is applied from the back chip side) and $2K_{NLtop}$ = 0.18 ± 0.09 %/FS (pressure is applied from the top chip side). All temperature characteristics have low errors, because the precision elements balance of PDA-NFL electric circuit was used. Additionally, the burst pressure is 80 times higher than the working range.

Keywords: pressure sensor, bipolar junction transistor, differential amplifier, high sensitivity, low error

1. Introduction

Microelectromechanical system (MEMS) piezoresistive pressure sensors with Wheatstone bridge electrical circuit are the most widely used elements for pressure analysis in many industrial and research fields. The silicon pressure sensor relevance is determined by small size, high output signal with low errors and mass fabrication. The chip area is “main price” which determines sensor output characteristics and its cost. The questions of balance between overall dimensions, complexity of fabrication processes, output sensitivity and low errors are most acute for sensor development of low-pressure ranges from 0.1 to 10.0 kPa, which are applicable in a wide range of industry, control systems (VAV) and medicine [1]. It is necessary that the low range pressure sensor chip provides high sensitivity limit. Sensitivity, in its turn, is a parameter which is limited by mechanical part of chip or membrane. The most influential geometric size of membrane is thickness of thinned membrane part, which will be reduced to a certain limit [2]. Subsequently, the thinned membrane part with thickness of several microns, where maximum mechanical stresses (MS) are created, is most susceptible to residual MS influence from: 1) SiO2 and Si3N4 layers, especially in case of their step distribution on top silicon surface [3,4], 2) metallization with significantly different coefficient of thermal expansion (CTE) [3-6], 3) the back surface roughness after etching [7], 4) types and methods of packaging [4,8-12]. These facts lead to error increase for nonlinearity, temperature characteristics and larger scatter of output parameters (especially without stop-

etching processes). Additionally, such structures with thinned membrane part are more susceptible to cracking or fracture during fabrication. Many developments consider the possibility of MS increase in piezoresistor (PR) areas by combinations of mechanical concentrator in the form of rigid islands (RIs) or complex shaped mechanical structures [13–20]. Such mechanical structures are created by using deep reactive ion etching (DRIE) of both back and top side of the chip. The use of DRIE is rather expensive process in mass production. Thus, the next most relevant parameter for membrane change is membrane area and, consequently, chip area. An expansion of chip area will increase pressure sensor cost.

The new promising method for pressure sensor sensitivity increase while maintaining or reducing dimensions is change of electrical circuit. The new electrical circuit with bipolar-junction transistor-based (BJT) piezosensitive differential amplifier with negative feedback loop (PDA-NFL) is applied. The efficiency of PDA-NFL circuit has already been successfully demonstrated for sensors of medium pressure range for 60 kPa [21,22].

2. PDA-NFL circuit analysis

The full theoretical model of PDA-NFL electrical circuit for pressure sensor chip, which was rather accurately confirmed by experimental research with detailed description of technological process, was presented in detail [23-25]. Therefore, only main results, applied in this development, will be indicated below. The article target is directed to detailed overview of developing of output characteristics with its beneficial proof in comparative analysis with pressure sensor analogs for 5 kPa.

The main advantage of PDA-NFL electrical circuit is combination possibility of 2 times more PRs p-type conductivity. It is possible due to the BJT three-pole contact connection. One of development directions of similar PDA-NFL electrical circuits is the use of deformable or non-deformable metal-oxide-semiconductor transistors (MOSFETs) or junction gate field-effect transistors (JFETs) instead of BJT and change of PDA-NFL electrical circuit to more complex combinations [26-32] in the future. The use of active elements complicates both the design and fabrication of pressure sensor chip because competent integration of MEMS and CMOS processes is necessary [33]. The PDA-NFL electrical circuit, in its turn, allows to use sensor in several applications without external amplification by ASIC or its gain reduction [34-37]. The ASIC connection for signal processing can be made in a similar way as connection with Wheatstone bridge, where the PRs for calibration is base divider resistance ($R_{b11,\ b21,\ b12,\ b22}$) in Figure 1. The specific location of PRs in the areas of compression or tension, as shown in Figure 1, and combination with BJT operation allows to distribute potentials and currents in the PDA-NFL

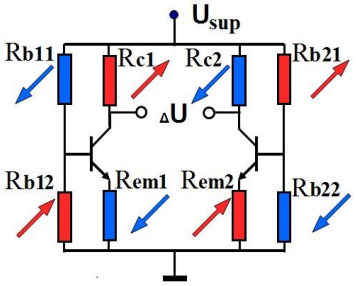

Figure 1. PDA-NFL electrical circuit with indicators of change direction for PRs when pressure is applied from the back side of chip.

circuit branches for more powerful output signal change of pressure than by using of Wheatstone bridge. The PDA-NFL output signal is potential difference of BJT collectors. The following main design issues were analyzed in previous works [22,24,25]:

- selection of BJT with vertical structure npn-type conductivity (V-NPN) or horizontal structure pnp-type conductivity (L-PNP);
- BJT location on deformable or non-deformable chip region;
- methods of topological and technological implementation of these electrical circuits with specific nominal element values to achieve a balance between high sensitivity and low temperature dependence;
- methods for noise component reduction of output signal which are caused by presence of active elements in electrical circuit.

The following most relevant applications of pressure sensor PDA-NFL were theoretically and experimentally proved:

- with BJT V-NPN structure relative to L-PNP analog, because the electrical circuit with BJT V-NPN has 1.54 times higher sensitivity and more compensated temperature characteristics (excluding the temperature coefficient of span). The BJT L-PNP structure disadvantages are probably caused by presence of parasitic current in substrate of emitter-epitaxial layer-substrate transistor. Sensitivity of pressure sensor chip PDA-NFL with effectively selected operating point of BJT V-NPN and PR resistance increases on average by 3.5 times relative to piezoresistive analogs with same mechanical part, which is optimally designed for certain ranges;
- with BJT location on non-deformable chip region (frame). The advantage of using the piezojunction effect [38-40] on BJT for different pressure ranges gives sensitivity increase only 1-5% in this electrical circuit. At the same time, the topological location of BJT with two PRs on small region is significantly complicated. The space-charge regions of neighboring circuit elements should not intersect

so the area of thinned membrane part, which is limited by volume between stress concentrators, will increase significantly. It will lead to MS decrease while other geometric parameters of membrane are saved;

- with BJT V-NPN structure relative to L-PNP analog, because the electrical circuit with BJT V-NPN has less noise component of output signal. The noise reduction is possible due to sufficient reducing of the influence of main component as Flicker noise, which is associated with generation and recombination of carrier effects in BJT active base region. The BJT active base region is shortened for achieving of high current gain.

3. Fabrication process

Pressure sensor chip PDA-NFL is created by silicon epitaxial structures (n – epitaxial layer, p – substrate) to isolate BJTs, which are located in a limited volume. The BJT fields are created by separation diffusion of the p^+ – conductivity type and substrate. The ground potential is applied to substrate. Electrical circuit elements are formed in the crystallographic plane (100) along the crystallographic direction [110]. The technological route for processing pressure sensor wafers:

1. Oxidation;
2. The sequence of cleaning, photolithography and doping steps, including:

a. boron for isolation areas and creating contact to the substrate;

b. boron for high-doped PR regions;

c. boron for low-doped PR regions and BJT base areas;

d. phosphorous for BJT emitter and collector areas;

3. Si_3N_4 deposition as protection layer for membrane etching;
4. Cavity photolithography on the back side of the wafer;
5. Wet anisotropic etching of membrane in 30% KOH aqueous solution at T = 85 °C;
6. Wet isotropic etching of membrane in a mixture of HF : HNO_3 : CH_3COOH (2:9:4);
7. Removal of Si_3N_4 layer;
8. Photolithography and etching to open contacts;
9. Sputtering of Al-Si (1.5%);
10. Photolithography and metal etching to define metal lines and bond pads;
11. Dicing

The chip membrane for 5 kPa range has a similar structure as other pressure sensor chip PDA-NFL. The mechanical part of chip as in cases of chip PDA-NFL development for other pressure ranges was created by KOH wet-etching with three RIs for MS concentration and linearity improvement. Geometrical parameters of membrane are shown in Figure 2(a) and Table 1. The presence of technological error due to disorientation of crystal orientation (100) and orientation flat [110] and error of combination for photo template along the orientation flat [41] are shown in Figure 2(a).

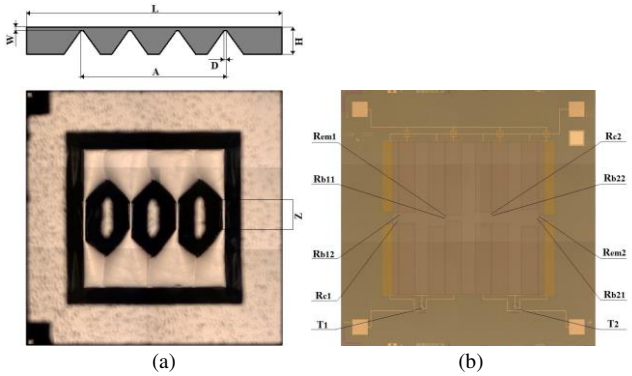

(a) (b)

Figure 2. Pressure sensor chip PDA-NFL: (a) back view and schematic image for cut of chip mechanical part with geometrical indicators; (b) top view with location indicators of all circuit elements.

Table 1. Geometrical parameters of pressure sensor chip PDA-NFL.

Geometrical Parameter	Size, μm
Chip side L	4000 ± 50
Thickness of tinned membrane part W	10 ± 2
Thickness of thickened membrane part H	400 ± 5
Membrane side A	2260 ± 15
Groove width between RIs or RI and chip frame D	23 ± 4
Length of RI edge Z	790 ± 60

The RI asymmetry, where average length of RI is 3 times more than length of the largest PRs $R_{b11, b21}$ (Figure 3), does not significantly influence output characteristics of membrane design for 5 kPa. During the creation of chip PDA-NFL membrane for different pressure ranges the variation between thickness of thinned membrane part W, RI edge length Z and width D of groove between the RIs or RI and chip frame appears. Topology of chip PDA-NFL has significant difference with Wheatstone bridge analogs, which have similar membrane with three RIs. Two PRs have to be placed in one of maximum MS regions as shown in Figure 2(b) and Figure 3 [22].

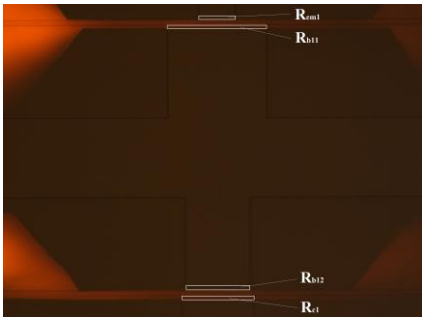

Figure 3. Photo of PRs (where R_{b11} is the longest element) location on thinned membrane part between RIs.

Metallization from a thin layer of aluminum (W_{Al} = 0.8 μm), which is necessary for PRs and BJT connection into electrical circuit, is located more than 80 μm from the edge of thinned membrane part. Connection between PRs and metallization occurs by high-doped p^+ - type regions, which have a low component of piezoresistor effect. The resistance contribution from high-doped p^+ - type regions was considered for getting of required balance for effective thermal compensation of circuit. Thus, full PR ratings consist of high-doped p^+ - type ($N_{sp+} = 7{,}4 \cdot 10^{19}$ cm^{-3}, $x_{jp+} = 3{,}6$ μm, $R_{sp+} = 17$ Ohm/cm^2) and low-doped p-type ($N_{sp-} = 8 \cdot 10^{18}$ cm^{-3}, $x_{jp-} = 1{,}8$ μm, $R_{sp-} = 200$ Ohm/cm^2) regions, where low-doped p-type regions make main contribution of piezoresistive effect [42-44]. All necessary input characteristics of BJT and PRs for operation of PDA-NFL electrical circuit are presented in Table 2. The chip PDA-NFL is created on a silicon wafers with diameter of 3 inches.

Table 2. Parameters of PDA-NFL electrical circuit.

Element	Parameter	Value
-	Supply voltage U_{sup}, V	5
BJT	Base current I_b, μA	4.6
	Gain β	145
	Base-emitter voltage ($U_b - U_{em}$), V	0.80
	Base-collector voltage ($U_c - U_b$), V	0.80
	Collector potential U_c, V	2.79
PR	$R_{b11, b21}$, kOhm	4.47
	$R_{b12, B22}$, kOhm	2.98
	$R_{c1, c2}$, kOhm	3.33
	$R_{em1, em2}$, kOhm	1.79

4. Output characteristics

Pressure sensor chip PDA-NFL was assembled into a silicon structure, which is placed on kovar case to analyze the output characteristics. The silicon construction of chip consists of intermediate element and pedestal, which are connected by low-temperature glass. The silicon construction connects with kovar case by organosilicon glue to reduce residual MS from case (Figure 4) [45–47]. Pads of pressure sensor chip connect to case pins by ultrasonic welding of aluminum wire. The sensor construction allows to measure differential pressure. The samples of pressure sensor chip PDA-NFL were divided into two groups. The first group (22 samples) has uniform supmembrane oxide (SO) over the thinned membrane part W_{SIO2} = 55 nm (Figure 2(b)). The second group (20 samples) doesn't have uniform SO and a whole surface isolation structure of the thinned membrane part is created after oxidation processes over different doping regions. Different thicknesses of SiO_2 steps from 0.18 to 0.42 μm was formed in second group. Creation of SO for the first group occurs after phosphorous diffusion by means of additional photolithography with followed thermal oxidation. All modes of previous doping process were corrected relatively second group without SO. Experimental groups were exposed to a temperature cycling and pressure cycling before measurements for removing of possible residual MS from silicon construction and case [45,48].

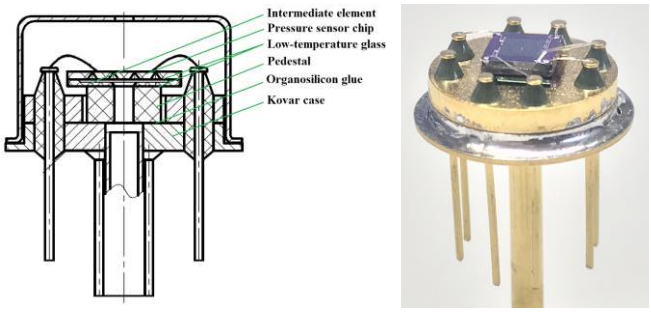

a) b)

Figure 4. Pressure sensor PDA-NFL assembly: (a) design drawing; (b) photo of sensor without upper part of case (cap).

Parametric characteristics for 5 kPa range are presented in the form of "arithmetic mean ± scatter as function of standard deviation". The measurements of zero signal, sensitivity, nonlinearity and noise component are considered at T = 23 °C. The measurements of each output signal for each sample are the arithmetic mean of 5 readings during 2.5 seconds. The reason for this measurement is high noise component of output signal. Sensitivity and nonlinearity by applying pressure from the back and top side of chip is calculated. Temperature characteristics are analyzed for two temperature ranges: "minus" -30...+20 °C and "plus" +20...+60 °C. The temperature characteristics and long-term stability (drift) are calculated as relative parameters to sensitivity, where pressure was applied from the back side of chip. The long-term stability of output signal was analyzed during the first 9 hours after power-up for chip electrical circuit. Overload pressure is carried out at pressure build-up speed of V_{burst} = 120 kPa/sec to check the mechanical strength. Output characteristics of pressure sensor PDA-NFL are shown in Table 3.

The next features between two groups are necessary to mark for analyzing the most relevant parameters of samples with SO (the first group):

- higher average sensitivity with smaller spread between samples S = 11.2 ± 1.8 mV/V/kPa;
- significantly smaller spread between the nonlinearity when pressure is applied from the back $2K_{NLback}$ = 0.11 ± 0.09 %FS and top $2K_{NLtop}$ = 0.18 ± 0.09 %FS side of chip (Figure 5);
- smaller errors of temperature characteristics, in particular for temperature hysteresis of zero signal.

Table 3. Output characteristics of pressure sensor PDA-NFL for 5 kPa.

Parameters	Detail	Value	
Type of chip		With SO	Without SO
Sensitivity S, mV/V/kPa	From back side	11.24 ± 1.81	10.01 ± 3.03
	From top side	11.23 ± 1.86	9.96 ± 2.97
Nonlinearity $2K_{NL}$, %FS	From back side	0.11 ± 0.09	0.08 ± 0.08
	From top side	0.18 ± 0.09	0.25 ± 0.19
Imbalance of zero output signal U_0, mV/V		< 8	
Noise of output signal U_{noise}, μV/V		3	
Temperature hysteresis of zero signal THZ, %FS/°C	–30…+20 °C	0.04 ± 0.02	0.11 ± 0.10
	+20…+60 °C	0.05 ± 0.03	0.12 ± 0.12
Temperature hysteresis of span THS, %FS/°C	–30…+20 °C	0.19 ± 0.05	0.21 ± 0.11
	+20…+60 °C	0.06 ± 0.04	0.07 ± 0.02
Temperature coefficient of zero signal TCS, %FS/10°C	–30…+20 °C	0.14 ± 0.08	0.25 ± 0.09
	+20…+60 °C	0.12 ± 0.08	0.20 ± 0.09
Temperature coefficient of span TCS, %FS/10°C	–30…+20 °C	2.22 ± 0.14	2.35 ± 0.19
	+20…+60 °C	2.04 ± 0.36	2.06 ± 0.30
Long-term stability (drift) U_{st}, %FS	Zero signal	0.03 ± 0.02	0,02 ± 0.02
	Sensitivity	0.02 ± 0.01	0,02 ± 0.01
Burst pressure P_{burst}, kPa		> 400	
Number of samples		22	20

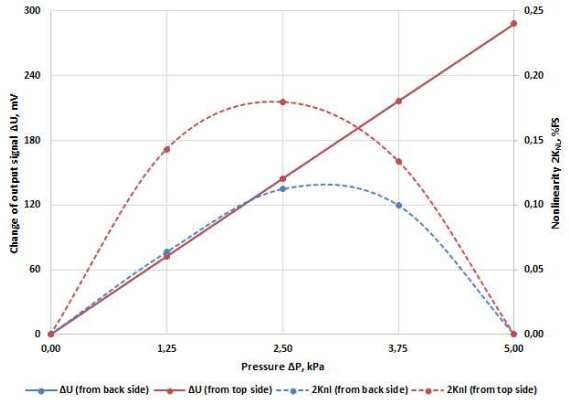

(a)

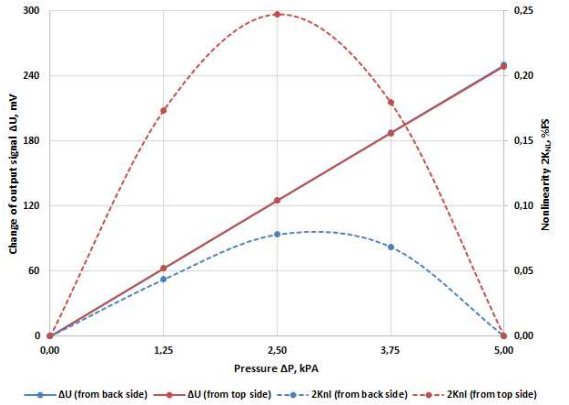

(b)

Figure 5. Dependence of zero output signal and nonlinearity on pressure for pressure sensor PDA-NFL: (a) with SO, (b) without SO.

5. Comparative analysis of pressure sensor with PDA-NFL and Wheatstone bridge electrical circuit

The first group of pressure sensor PDA-NFL with SO for comparative analysis with piezoresistive analogs utilizing Wheatstone bridge for 5 kPa is analyzed. 7 currently relevant works [49-55] from 4 research groups (according to the author opinion) were analyzed. The accurately detailed analysis of analog developments will be presented further. Table 4 shows all comparative characteristics of these works regarding pressure sensor PDA-NFL readings (articles [50,53] are marked by "*" represent only theoretical values). The calculation of parametric characteristics for pressure sensor PDA-NFL is presented as the most maximum for two options, when pressure is applied from top or back side of chip, the nonlinearity for this case is less than $2K_{NL}$ < 0.27 %FS. Important things were not analyzed from works, where the sensors were created for differential pressure:

- question of measurement symmetry, when pressure is applied from both sides of chip;
- temperature characteristics [56,57], which are no less important for pressure sensor than nonlinearity.

The balance relationship between high sensitivity and low nonlinearity for piezoresistive analogs is achieved by creating of new structure for mechanical part of chip (membrane) with actual location of PRs in this case.

The highest sensitivity was obtained in experimental development [49], where sensitivity of S = 5.14 mV/V/kPa, nonlinearity of $2K_{NL}$ = 0.28 %FS and membrane area of 2.90x2.90 mm^2. The presented pressure sensor PDA-NFL makes it possible to achieve 2.2 times higher sensitivity with similar nonlinearity and smaller element area. Additionally, pressure sensor PDA-NFL can reduce the mechanical hysteresis H by 8.7 times and the mechanical repeatability R by 6.6 times. Theoretical values in the paper [53] for similar membrane structure [49] indicate the possibility of sensitivity increasing to S = 6.93 mV/V/kPa and nonlinearity reducing $2K_{NL}$ = 0.23 %FS. Other experimental studies [51,52] with slightly lower nonlinearity of $2K_{NL}$ = 0.25 %FS and fairly high sensitivity were obtained. Comparative analysis of pressure sensor PDA-NFL with development [51] showed 2.4 times higher sensitivity with 4.0 times smaller membrane area. Additionally, pressure sensor PDA-NFL has 4.7 times lower mechanical hysteresis H and 2.4 times lower mechanical repeatability R. In the case of analysis with development [52] the sensitivity of pressure sensor PDA-NFL exceeds the indications by 2.5 times with slightly larger chip area by 24%. One of advantages for pressure sensor PDA-NFL is the mechanical strength, which is higher by 6.5 times. Nonlinearity of pressure sensor PDA-NFL are close to both cases because we must consider parameters within rather high spread which are presented on many chips.

Table 4. Comparative analysis of pressure sensor PDA-NFL with actual analogs utilizing piezoresistive Wheatstone bridge for 5 kPa.

Type of pressure sensor	Chip area, mm^2	Membrane area, mm^2	Membrane thickness, μm	Sensitivity S, mV/V/kPa	Nonlinearity $2K_{NL}$, %FS	Hysteresis H, %FS	Repeatability R, %FS	Zero signal U_0, mV/V	Burst pressure P_{burst}, kPa	Number of samples
PDA-NFL	4.00x4.00	2.26x2.26	10 ± 2	11.2 ± 1.8	< 0.27	0.03	0.08	< 8	> 400	22
CBMP [49]	-	2.90x2.90	12	5.14	0.28	0.26	0.53	1.6	-	-
PMNBCB [53]*	-	2.90x2.90	12	6.93	0.23	-	-	-	-	-
FBBM [51]	-	4.50x4.50	30	4.65	0.25	0.14	0.19	-	-	-
FBBM [50]*	-	4.50x4.50	30	5.10	0.75	-	-	-	-	-
CBP [52]	3.60x3.60	2.06x2.06	10	4.44	0.25	-	-	2.0	62	3
Peninsula [54]	3.60x3.60	1.90x1.90	10	3.68	0.36	-	-	0.4	-	2
CBM [55]	-	2.90x2.90	20	1.55	0.09	0.09	0.09	3.2	-	-

The other most relevant developments for this range have some lower sensitivity [54,55] or only mathematical model [50]. Additionally, it is necessary to note, that pressure sensor PDA-NFL relative to all chip design with Wheatstone bridge has:

• high mechanical strength, which exceeds P_{burst} > 400 kPa, without using stops [58-61];

• statistic data for comparative analysis with sufficiently large number of experimental samples;

• existence of relatively minor disadvantages, which are associated with increased imbalance of output signal U_0 < 8 mV/V and noise component of output signal U_{noise} < 3 μV/V. These disadvantages will able to compensated by ASIC;

• significantly higher sensitivity while thickness and area of thinned membrane part are saved.

6. Conclusion

Analysis of research results for pressure sensor with radically new electrical circuit PDA-NFL utilizing BJT V-NPN and SO for 5 kPa shows significant advantages that have been achieved relative to analogs of pressure sensors with piezoresistive Wheatstone bridge circuit for similar pressure range:

• sensitivity is 2.2 times higher ($S_{PDA\text{-}NFL}$ = 11.2 ± 1.8 mV/V/kPa) relative to the most sensitive analog [48] with similar error for nonlinearity ($2K_{NL\ PDA\text{-}NFL}$ < 0.27 %FS);

• area reduction of thinned membrane part (and most likely chip area) by 40% (chip PDA-NFL area 4.0x4.0 mm^2) relative to the most sensitive analog [48];

• high value of burst pressure $P_{burst\ PDA\text{-}NFL}$ > 400 kPa (80 times higher than the working range) without using of protective structure with stops;

• insignificant error of mechanical hysteresis $H_{PDA\text{-}NFL}$ = 0.03 %FS and mechanical repeatability $R_{PDA\text{-}NFL}$ = 0.08 %FS.

Experimental data of pressure sensor PDA-NFL measurement, which is created with and without SO, proved the influence of thickened step-formed isolation structure SiO_2 over the area of thinned membrane part. Pressure sensor PDA-NFL without SO has greater imbalance between two types of nonlinearity, when pressure is applied from the top and back sides of chip, significant sensitivity imbalance between sample data and higher errors of temperature characteristics, especially in temperature hysteresis of zero signal.

It is important to note that the pressure sensor PDA-NFL combination of selected electrical circuit and mechanical part with SO allows to achieve fairly low temperature dependence. The temperature characteristics for T = -30...+60 ^{0}C range, where the common parameter limits are regarded as the largest of two sub-ranges, have values: THZ < 0.08 %FS, THS < 0.24 %FS, TCZ < 0.22 %FS/10^{0}C and TCS < 2.4%FS/10^{0}C. Temperature characteristic errors have unilateral sign changes in 95% of cases. The imbalance between average values of nonlinearity, when pressure is applied from both sides of chip, is minimal enough $\Delta 2K_{NL\ PDA\text{-}NFL}$ = 0.07% FS. Long-term stability (drift) over 9 hours (T = 30 ^{0}C) is no more than U_{st} < 0.05 %FS. The pressure sensor PDA-NFL disadvantages are associated with two factors. The reason for high output signal imbalance is PDA-NFL circuit requirement for balance 2 times more PRs and additional 2 BJTs relative to Wheatstone bridge circuit. The noise component of output signal, which connected with BJT using, is no more than U_{noise} < 3 μV/V.

A potential direction for further development of pressure sensor for 5 kPa or lower ranges is application of PDA-NFL electrical circuit on the chip with advanced mechanical membrane structures, which were mentioned earlier.

Acknowledgements

The studies were financially supported by Dukhov All-Russia Research Institute of Automatics.

References

[1] Y. Charentenay, "MEMS Pressure Sensor Market and Technologies 2018," I-Micronews. Market & Technology report, 2018, pp. 28-31. [Online] Available: https://www.i-micronews.com/products/mems-pressure-sensor-market-and-technologies-2018/

[2] S. Timoshenko, S. Woinowsky-Krieger, "Theory of Plates and Shells," 2nd ed., New York, USA: McGraw-Hill, 1970, pp. 156-160.

[3] A.V. Tran, X. Zhang, B. Zhu, "Effects of temperature and residual stresses on the output characteristics of a piezoresistive pressure sensor," *IEEE Access*, vol. 7, pp. 27668-27676, 2019, DOI: 10.1109/ACCESS.2019.2901846.

[4] J.A. Chiou, S. Chen, "Thermal hysteresis analysis of MEMS pressure sensors," *Journal of Microelectromechanical Systems*, vol. 14, no. 4, pp. 782-787, 2005, DOI: 10.1109/JMEMS.2005.845460.

[5] Å. Sandvand, E. Halvorsen, H. Jakobsen, "In Situ Observation of Metal Properties in a Piezoresistive Pressure Sensor," *Journal of Microelectromechanical Systems*, vol. 26, no. 6, pp. 1381-1388, 2017, DOI: 10.1109/JMEMS.2017.2747090.

[6] H. San, Y. Li, Z. Song, Y. Yu, X. Chen, "Self-Packaging Fabrication of Silicon–Glass-Based Piezoresistive Pressure Sensor," *IEEE Electron Device Letters*, vol. 34, no. 6, pp. 789-791, 2013, DOI: 10.1109/LED.2013.2258320.

[7] H. Sandmaier, K. Kuhl, "A square-diaphragm piezoresistive pressure sensor with a rectangular central boss for low-pressure ranges," *IEEE Transactions on Electron Devices,* vol. 40, no. 10, pp. 1754-1759, 1993, DOI: 10.1109/16.277331.

[8] L.-T. Chen, J.-S. Chang, C.-Y. Hsu, W.-H. Cheng, "Fabrication and Performance of MEMS-Based Pressure Sensor Packages Using Patterned Ultra-Thick Photoresists," *Sensors*, vol. 9, no. 8, pp. 6200-6218, 2009, DOI: 10.3390/s90806200.

[9] R. Krondorfer, Y. K. Kim, J. Kim, C.-G. Gustafson, T. C. Lommasson, "Finite element simulation of package stress in transfer molded MEMS pressure sensors," *Microelectronics Reliability*, vol. 44, no. 12, pp. 1995-2002, 2004, DOI: 10.1016/j.microrel.2004.05.020.

[10] J.K. Reynolds, D. Catling, R. C. Blue, N. I. Maluf, T. Kenny, "Packaging a piezoresistive pressure sensor to measure low absolute pressures over a wide sub-zero temperature range," *Sensors and Actuators A: Physical,* vol. 83, no. 1-3, pp. 142-149, 2000, DOI: 10.1016/S0924-4247(00)00294-6.

[11] T.-L. Chou, C.-H. Chu, C.-T. Lin, K.-N. Chiang, "Sensitivity analysis of packaging effect of silicon-based piezoresistive pressure sensor," *Sensors and Actuators A: Physical,* vol. 152, no. 1, pp. 29-38, 2009, DOI: 10.1016/j.sna.2009.03.007.

[12] Y. Liu, H. Wang, W. Zhao, H. Qin, X. Fang, "Thermal-performance instability in piezoresistive sensors: Inducement and improvement," *Sensors,* vol. 16, no. 12, 1984, 2016, DOI: 10.3390/s16121984.

[13] P.K. Guo, J. King, M. Lester, R. Craddock, "A Hollow Stiffening Structure for Low-Pressure Sensors," *Sensors and Actuators A: Physical*, vol. 160, no. 1-2, pp. 35–41, 2010, DOI: 10.1016/j.sna.2010.03.024.

[14] L. Li, N. Belov, M. Klitzke, J-S. Park, "High Performance Piezoresistive Low Pressure Sensors," in *IEEE Sensors Conference,* Orlando, USA, 2016, pp. 1406-1408.

[15] M. Basov, D. Prigodskiy, "Investigation of High Sensitivity Piezoresistive Pressure Sensors at Ultra-Low Differential Pressures," *IEEE Sensors Journal*, vol. 20, no. 14, pp. 7646-7652, 2020, DOI: 10.1109/JSEN.2020.2980326.

[16] M. Basov, D. Prigodskiy, "Development of High-Sensitivity Piezoresistive Pressure Sensors for -0.5…+0.5 kPa," *Journal of Micromechanics and Microengineering*, vol. 30, no. 10, 105006, 2020, DOI: 10.1088/1361-6439/ab9581.

[17] C. Li, J. Xie, F. Cordovilla, J. Zhou, R. Jagdheesh, J. L. Ocaña, "Design, fabrication and characterization of an annularly grooved membrane combined with rood beam piezoresistive pressure sensor for low pressure measurements", Sensors and Actuators A: Physical, vol. 279, pp. 525-536, 2018, DOI: 10.1016/j.sna.2018.06.055.

[18] T. Xu, D. Lu, L. Zhao, Z. Jiang, H. Wang, X. Guo, Z. Li, X. Zhou, Y. Zhao, "Application and Optimization of Stiffness Abruption Structures for Pressure Sensors with High Sensitivity and Anti-Overload Ability", *Sensors*, vol. 17, no. 9, 1965, 2017, DOI: 10.3390/s17091965.

[19] B. Zhu, X. Zhang, Y. Zhang, S. Fatikow, "Design of diaphragm structure for piezoresistive pressure sensor using topology optimization," *Struct Multidisc Optim*, vol. 55, pp. 317–329, 2017, DOI: 10.1007/s00158-016-1470-x.

[20] X. Meng, Y. Zhao, "The Design and Optimization of a Highly Sensitive and Overload-Resistant Piezoresistive Pressure Sensor," *Sensors,* vol. 16, no. 3, 348, 2016, DOI: 10.3390/s16030348.

[21] M.V. Basov, D.M. Prigodskiy, "Investigation of a Sensitive Element for the Pressure Sensor Based on a Bipolar Piezotransistor," *Nano- and Microsystem Technology*, vol. 19, no. 11, pp. 685-693, 2017, DOI: 10.17587/nmst.19.685-693.

[22] M. Basov, "High-sensitivity MEMS pressure sensor utilizing bipolar junction transistor with temperature compensation," *Sensors and Actuators A: Physical,* vol. 303, 111705, 2020, DOI: 10.1016/j.sna.2019.111705.

[23] M.V. Basov, D.M. Prigodskiy, D.A. Holodkov, "Modeling of Sensitive Element for Pressure Sensor Based on Bipolar Piezotransistor," *Sensors and Systems*, vol. 6, pp. 17-24, 2017.

[24] M. Basov, "Development of High-Sensitivity Pressure Sensor with On-chip Differential Transistor Amplifier," *J. Micromech. Microeng.*, vol. 30, no. 6, 065001, 2020, DOI: 10.1088/1361-6439/ab82f1.

[25] M. Basov, "Ultra-High Sensitivity MEMS Pressure Sensor Utilizing Bipolar Junction Transistor for Pressures Ranging from -1 to 1 kPa," *IEEE Sensors Journal*, 2020, DOI: 10.1109/JSEN.2020.3033813.

[26] S. Hussain, P. Gnanachchelvi, J. C. Suhling, R. C. Jaeger, M. C. Hamilton, B. M. Wilamowski, "The Influence of Uniaxial Normal Stress on the Performance of Vertical Bipolar Transistors," in *Proceedings of the ASME 2013 International Technical Conference and Exhibition on Packaging and Integration of Electronic and Photonic Microsystems. Volume 1: Advanced Packaging; Emerging Technologies; Modeling and Simulation; Multi-Physics Based Reliability; MEMS and NEMS; Materials and Processes*, California., USA, 2013, V001T05A010.

[27] R.C. Jaeger, J.C. Suhling, R. Ramani, A. T. Bradley, J. Xu, "CMOS stress sensors on [100] silicon," *IEEE Journal of Solid-State Circuits*, vol. 35, no. 1, pp. 85-95, 2000, DOI: 10.1109/4.818923.

[28] V. Garcia, F. Fruett, "A mechanical-stress sensitive differential amplifier," *Sensors and Actuators A: Physical,* vol. 132, no. 1, pp. 8-13, 2006, DOI: 10.1016/j.sna.2006.06.060.

[29] X. Zhao, D. Wen, G. Li, "Fabrication and Characteristics of an nc-Si/c-Si Heterojunction MOSFETs Pressure Sensor," *Sensors*, vol. 12, no. 5, pp. 6369-6379, 2012, DOI: 10.3390/s120506369.

[30] Hafez, N., Haas, S., Loebel, K., D. Reuter, M. Ramsbeck, M. Schramm, J.T. Horstmann, T. Otto, "Characterisation of MOS Transistors as an Electromechanical Transducer for Stress," *Physica Status Solidi A*, vol. 216, no. 19, 1700680, 2018, DOI: 10.1002/pssa.201700680.

[31] P. Singh, J. Miao, L. Shao, R.K. Kotlanka, W.-T. Park, D.-L. Kwong, "Microcantilever sensors with embedded piezoresistive transistor read-out: Design and characterization," *Sensors and Actuators A: Physical,* vol. 171, no. 2, pp. 178-185, 2011, DOI: 10.1016/j.sna.2011.08.012.

[32] D. M. Stefanescu, "Handbook of Force Transducers Principles and Components," vol. 1, Berlin, Germany, Springer, 2011, pp. 136-152.

[33] M. Schwarz, "The Need of Simulation Methodologies for Active Semiconductor Devices in MEMS: Invited Paper," in *26th International Conference "Mixed Design of Integrated Circuits and Systems"*, Rzeszów, Poland, pp. 65-70, 2019.

[34] A.A. Barlian, W.T. Park, J.R. Mallon, A.J. Rastegar, B.L. Pruitt, "Review: Semiconductor piezoresistance for microsystems," *Proceedings of the IEEE*, vol. 97, no. 3, pp. 513–552, 2009, DOI: 10.1109%2FJPROC.2009.2013612.

[35] H. Baltes, O. Brand, A. Hierlemann, D. Lange, C. Hagleitner, "CMOS MEMS - present and future," in *MEMS 2002 IEEE International*

Conference. Fifteenth IEEE International Conference on Micro Electro Mechanical Systems, Las Vegas, USA, pp. 459-466, 2002.

[36] K. N. Bhat, M. N. Manjunatha, "MEMS Pressure Sensors-An Overview of Challenges in Technology and Packaging," *J. ISSS*, vol. 2, no. 1, pp. 39-71, 2013.

[37] A. Witvrouw, M. Gromova, A. Mehta, S. Sedky, P. Moor, K. Baert, C. Hoof, "Poly-SiGe, a superb material for MEMS", *MRS Proceedings*, vol. 782, A2.1, 2003, DOI: 10.1557/PROC-782-A2.1.

[38] F. Creemer, P.J. French, "A New Model of the Effect of Mechanical Stress on the Saturation Current of Bipolar Transistor," *Sensors and Actuators: A: Physical,* vol. 97-98, pp. 289-295, 2002, DOI: 10.1016/S0924-4247(01)00854-8.

[39] G. G. Babichev, S. I. Kozlovskiy, V. A. Romanov, N. N. Sharan, "Silicon pressure transducers with frequency output on base strain sensitive unijunction transistors," in *IEEE Sensors*, Orlando, USA, pp. 998-1001, 2002.

[40] F. Fruett, G.C.M. Meijer, "A New Sensor Structure Using the Piezojunction Effect in PNP Lateral Transistor," *Sensors and Actuators: A: Physical,* vol. 92, no. 1-3, pp. 197-202, 2001, DOI: 10.1016/S0924-4247(01)00563-5.

[41] V. Lindroos, M. Tilli, A. Lehto, T. Motooka, "Handbook of Silicon Based MEMS Materials and Technologies," vol. 1, Oxford, England, William Andrew Applied Science Publishers, 2010, pp. 203-209.

[42] C. Cho, R. C. Jaeger, J. C. Suhling, "Characterization of the Temperature Dependence of the Piezoresistive Coefficients of Silicon From -150 ^{0}C to +125 ^{0}C," *IEEE Sensors Journal*, vol. 8, no. 8, pp. 1455-1468, 2008, DOI: 10.1109/JSEN.2008.923575.

[43] J. Richter, J. Pedersen, M. Brandbyge, E. V. Thomsen, O. Hansen, "Piezoresistance in p-type silicon revisited," *Journal of Applied Physics*, vol. 104, no. 5, 023715, 2008, DOI: 10.1063/1.2960335.

[44] A. Masolin, P. Bouchard, R. Martini, M. Bernacki, "Thermo-mechanical and fracture properties in single-crystal silicon," *J Mater Sci,* vol. 48, pp. 979–988, 2013, DOI: 10.1007/s10853-012-6713-7.

[45] Å. Sandvand, E. Halvorsen, K. E. Aasmundtveit, H. Jakobsen, "Identification and Elimination of Hygro-Thermo- Mechanical Stress-Effects in a High-Precision MEMS Pressure Sensor," *Journal of Microelectrome*chanical Systems, vol. 26, no. 2, pp. 415-423, 2017, DOI: 10.1109/JMEMS.2017.2651162.

[46] M. S. Zarnik, D. Rocak, S. Macek, "Residual stresses in a pressure-sensor package induced by adhesive material during curing: a case study," *Sensors and Actuators A: Physical,* vol. 116, no. 3, pp. 442-449, 2004, DOI: 10.1016/j.sna.2004.05.010.

[47] J. Wang, X. Li, "Package-friendly piezoresistive pressure sensors with on-chip integrated packaging-stress-suppressed suspension (PS3) technology," *J. Micromech. Microeng.*, vol. 23, no. 4, 045027, 2013, DOI: 10.1088/0960-1317/23/4/045027.

[48] K. Birkelund, P. Gravesen, S. Shiryaev, P. B. Rasmussen, M. D. Rasmussen, "High-pressure silicon sensor with low-cost packaging," *Sensors and Actuators A: Physical,* vol. 92, no. 1-3, pp. 16-22, 2001, DOI: 10.1016/S0924-4247(01)00534-9.

[49] A. V. Tran, X. Zhang, B. Zhu, "The Development of a New Piezoresistive Pressure Sensor for Low Pressures," *IEEE Transactions on Industrial Electronics*, vol. 65, no. 8, pp. 6487-6496, 2018, DOI: 10.1109/TIE.2017.2784341.

[50] C. Li, F. Cordovilla, R. Jagdheesh, J.L. Ocana, "Design and optimization of a novel structural MEMS piezoresistive pressure sensor," *Microsyst Technol,* vol. 23, pp. 4531–4541, 2017, DOI: 10.1007/s00542-016-3187-6.

[51] C. Li, F. Cordovilla, R. Jagdheesh, J.L. Ocana, "Design Optimization and Fabrication of a Novel Structural SOI Piezoresistive Pressure Sensor with High Accuracy," *Sensors*, vol. 18, no. 2, 439, 2018, DOI: 10.3390/s18020439.

[52] X. Huang, D. Zhang, "Structured diaphragm with a centre boss and four peninsulas for high sensitivity and high linearity pressure sensors," *Micro and Nano Letters*, vol. 9, no. 7, pp. 460-463, 2014, DOI: 10.1049/mnl.2014.0154.

[53] Tran, A.V., Zhang, X., Zhu, B., "Mechanical Structural Design of a Piezoresistive Pressure Sensor for Low-Pressure Measurement: A Computational Analysis by Increases in the Sensor Sensitivity," *Sensors*, vol. 18, no. 7, 2023, 2018, DOI: 10.3390/s18072023.

[54] X. Huang, D. Zhang, "High Sensitive and Linear Pressure Sensor for Ultra-low Pressure Measurement," *Procedia Engineering*, vol. 87, pp. 1202-1205, 2014, DOI: 10.1016/j.proeng.2014.11.383.

[55] B. Tian, Y. Zhao, Z. Jiang, B. Hu, "The design and analysis of beam-membrane structure sensors for micro-pressure measurement," *Review of Scientific Instruments*, vol. 83, no. 4, 045003, 2012, DOI: 10.1063/1.3702809.

[56] M. Aryafar, M. Hamedi, M.M. Ganjeh, "A novel temperature compensated piezoresistive pressure sensor," *Measurement*, vol. 63, pp. 25-29, 2015, DOI: 10.1016/j.measurement.2014.11.032.

[57] G. Zhou, Y. Zhao, F. Guo, W. Xu, "A Smart High Accuracy Silicon Piezoresistive Pressure Sensor Temperature Compensation System," *Sensors*, vol. 14, no. 7, pp. 12174-12190, 2014, DOI: 10.3390/s140712174.

[58] D.M. Prigodskiy, M.V. Basov, "Research of Pressure Sensitive Elements with Increased Strength," *Nano- and Microsystem Technology*, vol. 21, no. 6, pp. 368-376, 2019, DOI: 10.17587/nmst.21.368-376.

[59] L. Christel, K. Petersen, P. Barth, F. Pourahmadi, J. Mallon, J. Bryzek, "Single-crystal Silicon Pressure Sensors with 500x Overpressure Protection," *Sensors and Actuators A: Physical*, vol. 2, no. 1-3, pp. 84-88, 1990, DOI: 10.1016/0924-4247(90)85017-X.

[60] T. Kober, R. Werthschützky, "Wafer Level Processing of Overload-Resistant Pressure Sensors," *Procedia Engineering*, vol. 47, pp. 615-618, 2012, DOI: 10.1016/j.proeng.2012.09.222.

[61] J. Auersperg, E. Auerswald, C. Collet, Th. Dean, D. Voge, Th. Winkler, S. Rzepka, "Effects of residual stresses on craclring and delamination risks of an avionics MEMS pressure sensor," in 1*8th Intemational Conference on Thermal, Mechanical and Multi-Physics Simulation and Experiments in Microelectronics and Microsystems*, Dresden, German, pp. 1-5, 2017.